ЯДЕРНА ФІЗИКА ТА ЕНЕРГЕТИКА / NUCL. PHYS. AT. ENERGY 24 (2023) 193-208 ISSN 1818-331X

УДК 539.165 https://doi.org/10.15407/jnpae2023.03.193

P. Belli[1,2], R. Bernabei[1,2,*], F. Cappella[3,4], V. Caracciolo[1,2], R. Cerulli[1,2], F. A. Danevich[2,5], A. Inchicchitti[3,4], D. V. Kasperovych[5], V. R. Klavdiienko[5], V. V. Kobychev[5], A. Leoncini[1,2], V. Merlo[1,2], O. G. Polischuk[3,5], V. I. Tretyak[5,6]

[1] *Department of Physics, University of Rome "Tor Vergata", Rome, Italy*
[2] *National Institute for Nuclear Physics, "Tor Vergata", Rome, Italy*
[3] *National Institute for Nuclear Physics, Rome, Rome, Italy*
[4] *Department of Physics, University of Rome "La Sapienza", Rome, Italy*
[5] *Institute for Nuclear Research, National Academy of Sciences of Ukraine, Kyiv, Ukraine*
[6] *National Institute for Nuclear Physics, Gran Sasso National Laboratory, Assergi, Italy*

*Corresponding author: rita.bernabei@roma2.infn.it

LOW-BACKGROUND EXPERIMENT TO SEARCH FOR DOUBLE BETA DECAY OF ^{106}Cd USING ^{106}CdWO$_4$ SCINTILLATOR

An experiment to search for 2ε-, εβ$^+$- and 2β$^+$-decays of ^{106}Cd, using a 215 g cadmium tungstate scintillation crystal enriched at 66 % by ^{106}Cd (^{106}CdWO$_4$) is carried out at the Gran Sasso underground laboratory (Italy). Events in the ^{106}CdWO$_4$ detector are recorded in (anti)coincidences with two large-volume CdWO$_4$ scintillation counters. The design of the detector system, calibration and background measurements, methods, and results of data analysis to determine key detector characteristics are described. The experimental data are compared with Monte Carlo simulation results, and a background model is constructed. The radioactive contamination of the setup components is studied. The sensitivity of the experiment approaches the level of theoretical predictions for the 2νεβ$^+$-decay channel, while for other possible 2β-decay channels it is already on the level of lim $T_{1/2}$ ~ 10^{21} - 10^{22} years.

Keywords: ^{106}Cd, double beta decay, 2ε, εβ$^+$, 2β$^+$, low background, scintillation detector.

1. Introduction

The existence of neutrino oscillations testifies a non-zero mass for this elementary particle, which requires an extension of the Standard Model (SM) of particle physics. However, oscillation experiments cannot answer questions about the nature of neutrinos (whether they are Dirac or Majorana particles), determine the absolute mass and neutrino mass hierarchy. One of the most promising ways to study the properties of the neutrino is the double beta (2β) decay of atomic nuclei. It changes the nuclear charge by two units: (A, Z) → (A, Z ± 2) [1 - 3]. Different types of the process are possible with emission/absorption of electrons and positrons. The two-neutrino (2ν2β) mode of the process is allowed by the SM but strongly suppressed. The neutrinoless 2β-decay (0ν2β) violates the lepton number conservation and is possible if the neutrino is a Majorana particle (a fermion that is identical to its antiparticle). Being a process beyond the SM, 0ν2β-decay is one of the best approaches to test the SM [4 - 7]. Furthermore, the Majorana nature of the neutrino may shed light on the problem of the baryon asymmetry of the Universe [8, 9].

The two-neutrino mode of the 2β-decay has been observed in several nuclides [10, 11]. This decay has the longest half-life among all known radioactive transitions: 10^{18} - 10^{24} years. The 0ν2β-process has never been observed, the most sensitive experiments provide only lower half-life limits at the level of $T_{1/2} > 10^{24}$ - 10^{26} years. It should be noted that all 2β-decays that have been clearly detected were transitions with the emission of two electrons (2ν2β$^-$). As for the allowed two-neutrino "2β-plus decays": double electron capture (2ε), double positron emission (2β$^+$), and electron capture with positron emission (εβ$^+$), there are only indications of 2ε-decay in three nuclides: ^{130}Ba, ^{78}Kr and ^{124}Xe. Signs of the 2ν2ε-decay of ^{130}Ba were found in two geochemical experiments, where an anomaly in the isotopic concentration of daughter xenon was observed in old barite minerals (BaSO$_4$), which was interpreted as the double electron capture with $T_{1/2}$ = (2.16 ± 0.52) × × 10^{21} years [12] and $T_{1/2}$ = (6.0 ± 1.1)·10^{20} years [13]. An indication on the 2ν2ε-decay of ^{78}Kr was claimed in an experiment using a proportional counter with a volume of 49 l, filled with 99.81 % of enriched ^{78}Kr isotope [14]. The value of the half-life was updated as $T_{1/2}$ = $1.9^{+1.3}_{-0.8}$·10^{22} y [15]. Recently, the observation of 2ν2ε-decay of ^{124}Xe with $T_{1/2}$ = (1.18 ± 0.19) × × 10^{22} years was reported in the XENON dark matter search experiment [16]. However, the 2ε-decay of ^{130}Ba needs to be confirmed n direct detector experiments, while the results for ^{78}Kr and ^{124}Xe are awaiting confirmation in independent measurements with larger statistics. Other allowed "2β-plus decays" modes, $2\nu\varepsilon\beta^+$ and $2\nu2\beta^+$, have not yet been observed.

^{106}Cd is one of the most attractive candidates to search for 2ε-, $\varepsilon\beta^+$-, and $2\beta^+$-decays with a long history of studies. A simplified decay scheme of ^{106}Cd is shown in Fig. 1. A review of previous studies can be found in [17]. ^{106}Cd has one of the highest decay energies, $Q_{2\beta}$ = 2775.39(10) keV [18], a relatively high isotopic abundance δ = 1.245(22) % [19], and a possibility of a large-scale enrichment using gas centrifugation. It is important that methods of purification and production of high-quality cadmium tungstate crystal scintillators are well developed.

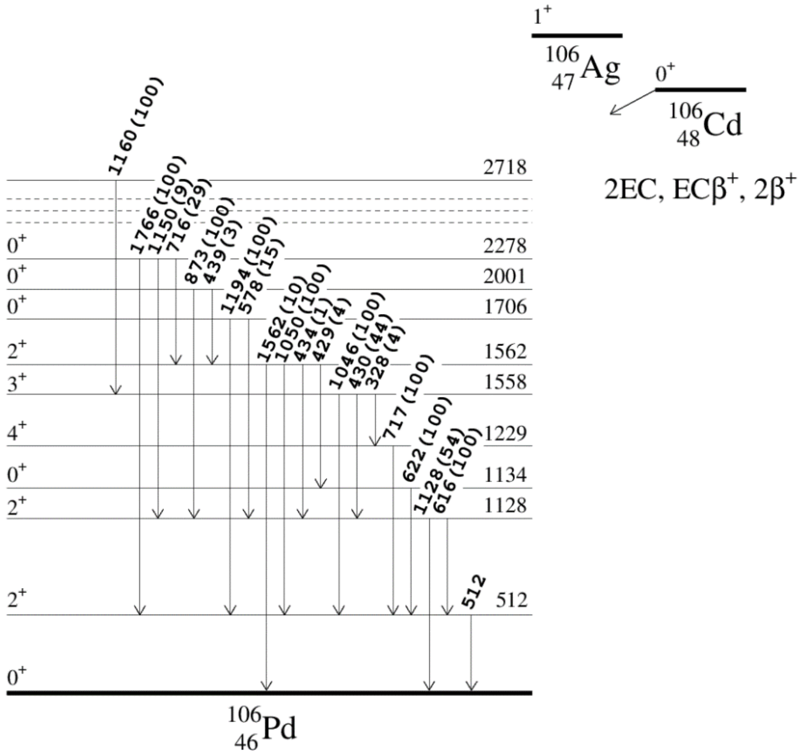

Fig. 1. A simplified scheme of 2β-decay of ^{106}Cd (excitation energies in the interval 2283 - 2714 keV are omitted). The energies of excited levels are given in keV. Relative intensities of γ-ray transitions are given in parentheses [23].

For this study, a near cylindrical cadmium tungstate crystal (approximate dimensions Ø27 mm × × 50 mm) with a mass of 215.4 g, enriched in the ^{106}Cd isotope to 66 % ($^{106}CdWO_4$) was developed in 2010 [20]. Previous experiments using this crystal provided limits on the half-life of ^{106}Cd for different decay channels and modes at the level of $T_{1/2} \geq 10^{20}$ - 10^{21} years [17, 21, 22].

2. Experiment

2.1. Experimental setup

An experiment using the $^{106}CdWO_4$ crystal is carried out at the Gran Sasso underground laboratory of the National Institute for Nuclear Physics (LNGS, Italy) at a depth of 3.6 km of water equivalent. Fig. 2 shows a schematic diagram of the setup.

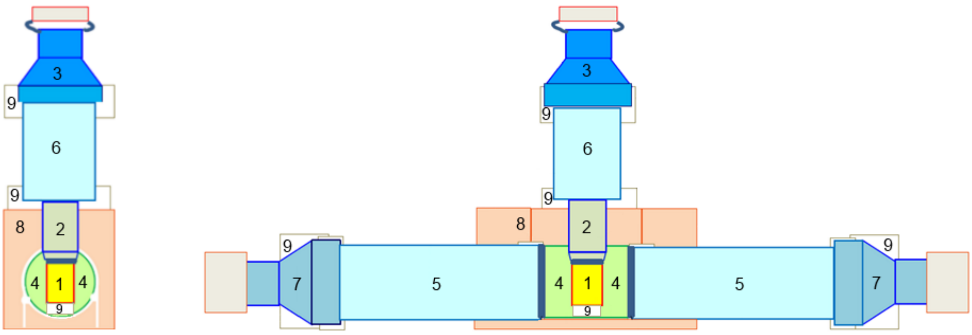

Fig. 2. Schematic diagram of the experimental setup with the $^{106}CdWO_4$ detector. The $^{106}CdWO_4$ crystal scintillator (*1*) is viewed through a plastic scintillator (*2*) and a quartz light-guide (*6*) by a photomultiplier (*3*). Two $CdWO_4$ crystal scintillators (*4*) are viewed through quartz light-guides (*5*) by photomultipliers (*7*). The three detectors were surrounded by high-purity copper shielding (*8*). Teflon details (*9*) were used to fix the positions of the detector system details. (See color Figure on the journal website.)

The $^{106}CdWO_4$ scintillator was surrounded by two $CdWO_4$ crystal scintillators with dimensions of Ø70 mm × 38 mm, with semi-cylindrical holes to tightly enclose the enriched crystal. The central detector was viewed by a low radioactivity photomultiplier tube (PMT) Hamamatsu R11065-20MOD through a quartz light-guide (Ø66 mm × 100 mm) and a polystyrene-based plastic scintillator (Ø40 mm × 83 mm). Both the $CdWO_4$ crystal scintillators were viewed by Hamamatsu R6233MOD PMTs through light-guides made of high-purity quartz (Ø70 mm × 200 mm). All the optical contacts between the detector details were provided with optical grade silicone grease EJ-550 by Eljen Technology. The detectors were wrapped in Teflon tape and aluminized plastic film to improve the light collection. To ensure optical contact of the $^{106}CdWO_4$ detector with the light-guide, a Teflon spring was inserted. The detectors were surrounded by high-purity copper shielding ("internal copper") with a thickness of 1 - 7 cm. To reduce the external radiation background, the entire detector setup was surrounded by layers of ultra-pure copper ("external copper", 11 cm), lead (10 cm), a layer of cadmium (2 mm) and polyethylene and paraffin plates (10 cm) to absorb thermal neutrons. Photographs of the experimental setup are shown in Fig. 3. To remove radon, the inner volume of the setup was flushed with high-purity nitrogen gas. The upper limit of radon concentration in the nitrogen is $< 5.8 \cdot 10^{-2}$ Bq/m^3 (with a 90 % confidence level) [24].

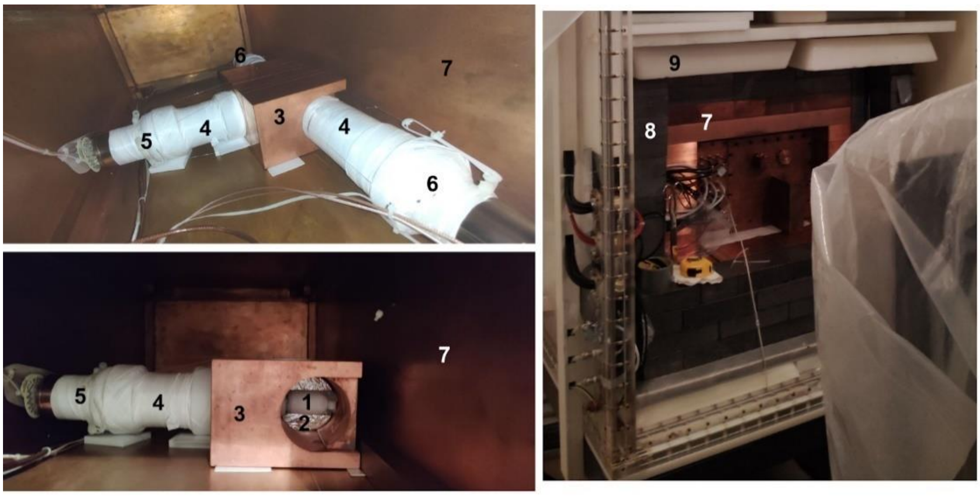

Fig. 3. Photograph of the experimental setup (a part of the passive shield is disassembled). $^{106}CdWO_4$ crystal scintillator (*1*), one of the $CdWO_4$ crystal scintillator (*2*), "inner copper" (*3*), quartz light guides (*4*), Hamamatsu R11065-20MOD photomultiplier (*5*), Hamamatsu R6233MOD photomultipliers (*6*), "external copper" (*7*), lead shield (*8*), paraffin plates (*9*). (See color Figure on the journal website.)

The detection system was connected to an 8-bit transient digitizer with a sampling frequency of 1 GSample/s (DC270 from Agilent Technology) and a bandwidth of 250 MHz. The event-by-event data acquisition system recorded the pulse shape of each event within a 100 μs time window and its arrival time. The $^{106}CdWO_4$ crystal scintillator contains β-active nuclides: natural ^{113}Cd and radiogenic ^{113m}Cd. Their decays provide the main part of events rate at low energies. To reduce the data flow from β-decays of ^{113}Cd and ^{113m}Cd, the energy threshold of the electronic system that produces the trigger was set at ≈ 0.5 MeV for events in anticoincidence. For events in coincidence with the $CdWO_4$ counters, the trigger threshold for $^{106}CdWO_4$ was set at ≈ 0.05 MeV. The thresholds for the $CdWO_4$ scintillation counters were set at ≈ 0.03 MeV. Thus, the data acquisition system recorded events when one of the two conditions was fulfilled:

– an individual event in $^{106}CdWO_4$ with energy higher than ≈0.5 MeV;

– an event with energy higher than ≈ 0.05 MeV in the $^{106}CdWO_4$ in coincidence with an event with energy higher than ≈ 0.03 MeV in at least one of the $CdWO_4$ counters.

The detection system was calibrated at the beginning, in the middle, and at the end of the experiment using γ-sources ^{22}Na, ^{60}Co, ^{133}Ba, ^{137}Cs, and ^{228}Th, which allowed determining the energy scale, energy resolution of the detectors and tracking their stability over time.

2.2. Spectrometric and time characteristics of the detector system

The energy resolution of the $^{106}CdWO_4$ detector can be described by the function FWHM (keV) = $= 4.56 \cdot \sqrt{E_\gamma}$, where E_γ is the energy of γ-ray quanta in keV. For the two $CdWO_4$ counters, the energy resolution was estimated as FWHM = $\alpha \cdot \sqrt{E_\gamma}$, with α-coefficients equal to 2.95 and 2.72. The energy scale of the detectors (mainly of the $^{106}CdWO_4$ one) was changed during the experiment. It can be associated with gain degradation of the detectors PMTs. The effect was taken into account in the estimations of the detector's energy resolutions and thresholds in the whole data.

The energy scale time shift of the $^{106}CdWO_4$ detector was estimated using the edge of the ^{113m}Cd β-spectrum and the results of the calibration measurements. To approximate the β-spectrum edge, the following formula was used:

$$f(E) = A\int_0^{Q'_\beta} \rho(E')R(E,E')dE', \qquad (1)$$

where A is the amplitude; Q'_β is the parameter of the approximation representing the β-spectrum edge; $\rho(E)$ is the energy distribution of the emitted electron; $R(E,E')$ is the energy resolution, which is described by a Gaussian function:

$$R(E,E') = \frac{1}{\sqrt{2\pi}\sigma(E')} exp\left(\frac{-(E-E')^2}{2\sigma^2(E')}\right). \qquad (2)$$

The energy distribution of an emitted electron in a β-decay can be described by the formula $\rho(E) = wpF(E,Z)(Q'_\beta - E)^2 C(w)$, where $w = 1 + E/m_e c^2$, m_e is a mass of an electron, p is the electron momentum, $F(E,Z)$ is the Fermi function, Z is the charge of the daughter nucleus and $C(w)$ is a correction factor. For the first forbidden non-unique β decays, as ^{113m}Cd, $C(w) = 1$ is a good approximation [25]. Taking the Primakoff - Rosen approximation $F(E,Z) \sim w/p$ [26] we obtain the simplified formula used in this analysis:

$$\rho(E) = \left(w(Q'_\beta - E)\right)^2. \qquad (3)$$

An example of ^{113m}Cd β spectrum approximation measured by the $^{106}CdWO_4$ detector is shown in Fig. 4. One can see that there is a β spectrum edge shift, which is associated with a decrease in the PMT gain. Differences in the shape of the spectrum are due to the fact that at the beginning of the experiment, the data were collected for several days with a low-energy trigger (see Fig. 4, *a*). Therefore, the maximum in the spectrum at ~ 450 a.u. in Fig. 4, *b* is due to the use of a higher energy value for the trigger of the $^{106}CdWO_4$ detector.

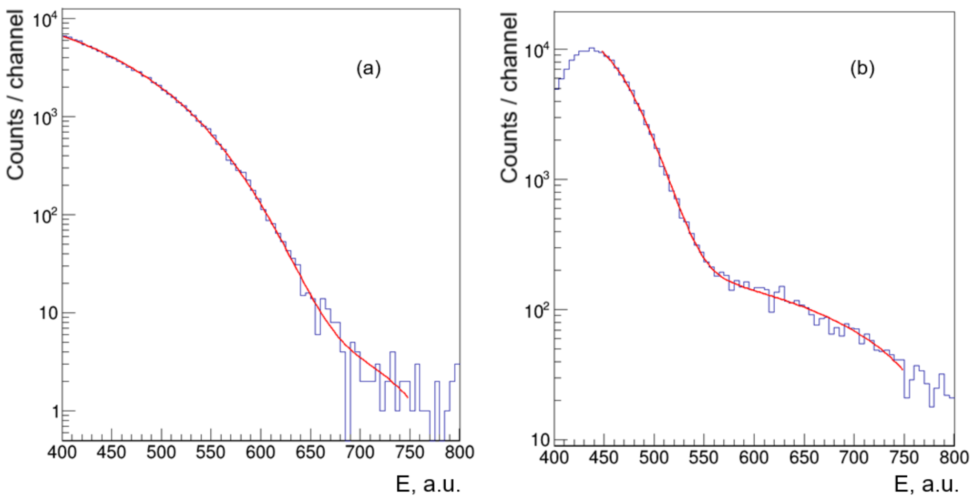

Fig. 4. Energy spectra collected by the $^{106}CdWO_4$ detector in the first days of the experiment (*a*) and after ~ 240 days (*b*). The red line represents an approximation of the β-spectrum edge of ^{113m}Cd with function (*1*) plus a linear function to describe the background. The maximum in the spectrum (*b*) at ~ 450 a.u. is a threshold effect associated with the operation of the electronics to produce hardware trigger. (See color Figure on the journal website.)

The dynamics of the ^{113m}Cd β-spectrum shift is shown in Fig. 5 (the jump in the β-spectrum edge after 380 days is caused by an increase in the high voltage applied to the PMT). Similar degradation of the PMT gain is observed in many experiments [27 - 29] and can be described by a sum of several exponentials. The gain degradation was also estimated by using the calibration results. To compensate the energy shift, the energy value of each event recorded by the $^{106}CdWO_4$ detector was divided by the degradation function $D(t)$. Overall, the shift in the energy scale over the data acquisition time t in days was determined as $D_1(t) = 0.82 \cdot exp\left(\frac{-t}{2221}\right) + 0.18 \cdot exp\left(\frac{-t}{41}\right)$ and $D_2(t) = exp\left(\frac{-t}{3002}\right)$ for the data before and after the high voltage increase, respectively.

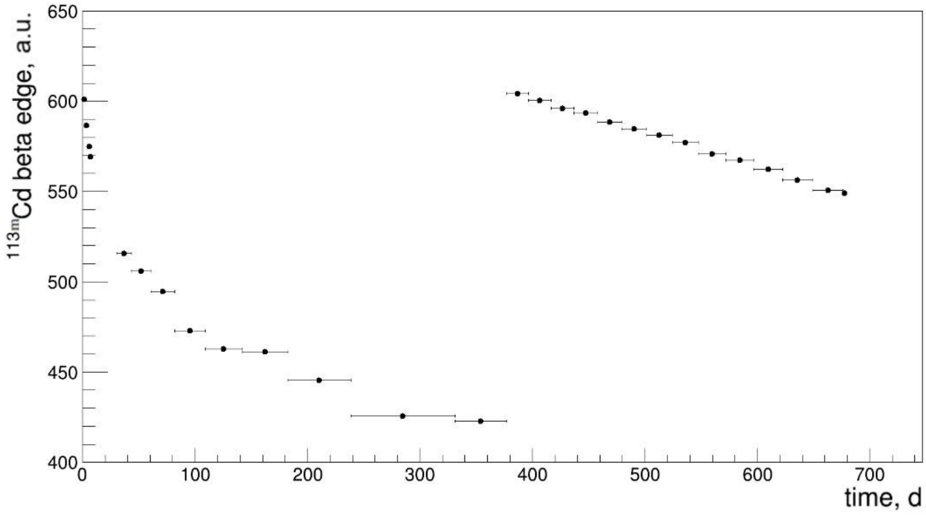

Fig. 5. Dependence of the β-spectrum edge of ^{113m}Cd on time, due to the gain degradation of the $^{106}CdWO_4$ PMT. The jump in the value of the β-spectrum edge after 380 days is caused by an increase in the high voltage on the PMT.

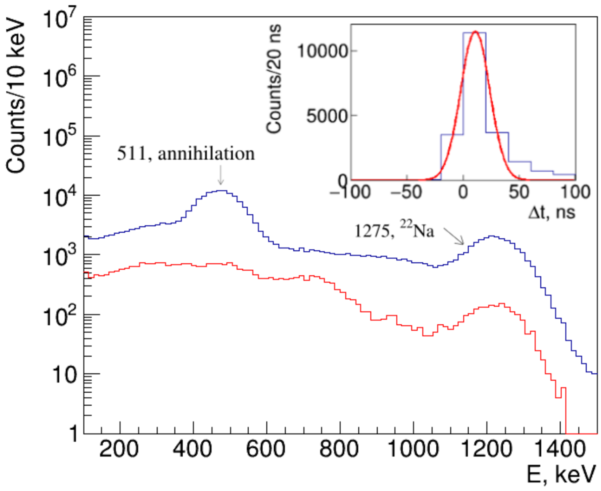

Fig. 6. The energy spectrum of γ-ray quanta of the ^{22}Na source measured by the $^{106}CdWO_4$ detector. The blue line represents the spectrum without cuts, while the red line shows coincidences with an event with an energy of 511 ± σ keV in at least one of the $CdWO_4$ detectors. The energies of the γ-quanta are given in keV. The inset shows the time distribution of the initial positions of the $^{106}CdWO_4$ detector pulses relative to the signals from the $CdWO_4$ counters with energy 511 ± σ keV. (See color Figure on the journal website.)

The time resolution of the detector system was determined using calibration with the ^{22}Na γ-source. Fig. 6 shows spectra collected by the $^{106}CdWO_4$ detector with the ^{22}Na source, without cuts and in coincidence with events with energy of 511 ± 1σ keV in at least one of the $CdWO_4$ counters, where σ is the energy resolution of the $CdWO_4$ counters for 511 keV γ-ray quanta. The insert in Figure shows the distribution of time intervals between the start of pulses in the $^{106}CdWO_4$ detector and signals in the $CdWO_4$ counters with an energy of 511 ± 1σ keV, with a standard deviation of 13 ns.

2.3. Comparison of the experimental data obtained with γ-sources to Monte Carlo simulations

We have compared the experimental data obtained in the calibration runs with γ-ray sources and distributions simulated by the Monte Carlo package EGSnrc [30]. The comparison allowed also to refine energy thresholds and verify the performance of the coincidence mode of the detector system. The ^{228}Th source was chosen because it had a sufficiently high activity (6.1 ± 0.3 kBq) and a wide energy range of γ-ray quanta. Fig. 7 shows a comparison between the spectrum measured with the ^{228}Th source (with background subtraction) and the simulated model. Approximately 30 million events were simulated. Comparing the experimental spectrum with the model, the high energy threshold of 467 ± 40 keV was determined for the individual events in $^{106}CdWO_4$ when energy deposition in $CdWO_4$ counters was lower than their energy thresholds (see Fig. 7, *a* cyan histogram), and low energy threshold of 52 ± 12 keV for events in the $^{106}CdWO_4$ detector in coincidences with the $CdWO_4$ detectors (see Fig. 7, *a* blue histogram). Meanwhile, the energy thresholds of the $CdWO_4$ counters were determined as 46 ± 2 keV and 32 ± 2 keV. The approximation of the spectrum with the model gives a value of the source activity of 5.70 ± 0.01 kBq which reasonably agrees with the specification of the source.

The comparison of data and the Monte Carlo model also allowed checking the operation of the data acquisition system in the different coincidence (anticoincidence) modes. Fig. 8 shows a comparison between the data measured by the $^{106}CdWO_4$ detector and the simulated model in anticoincidence mode (*a*), in coincidence with the event(s) in the $CdWO_4$

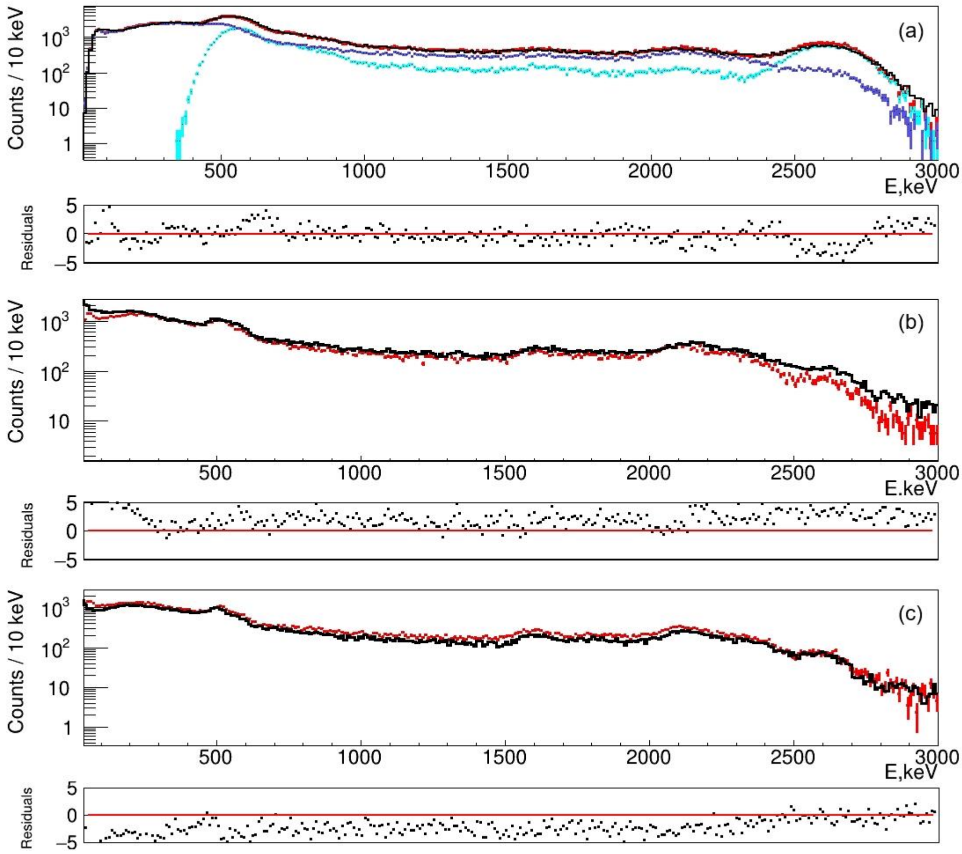

Fig. 7. Energy spectra of ^{228}Th γ-ray source measured by $^{106}CdWO_4$ (*a*) and $CdWO_4$ (*b*, *c*) detectors (black histograms), when no cuts are applied. Monte Carlo models are shown by red markers. The cyan Monte Carlo model represents individual events in $^{106}CdWO_4$ and the blue one is events in the $^{106}CdWO_4$ detector in coincidence with the $CdWO_4$ counters. The residual distributions defined as (experiment – model)/uncertainties are shown below each spectrum. (See color Figure on the journal website.)

counters (*b*), in coincidence with the event(s) in at least one of the $CdWO_4$ counters with the energy release E = 511 ± 2σ keV (*c*) and in coincidence with the events in both the $CdWO_4$ counters with energy E = 511 ± 2σ keV (*d*), where σ is the energy resolution of the $CdWO_4$ counters. The simulations reasonably represent the data above 0.45 MeV in the anticoincidence spectrum and above 0.05 MeV in coincidence spectra that correspond to the hardware energy thresholds of the $^{106}CdWO_4$ detector.

Some inconsistency between the experimental and simulated spectra can be explained by uncertainties of the positions and activity of the source, by simplification of the set-up geometry used for the Monte Carlo simulations, the uncertainty of the energy resolution of the detectors, and some instability of the detector system during the calibration. Additionally, the background was not taken into account in the simulations.

3. Data analysis

3.1. Pulse-shape discrimination

The difference in the scintillation signal shape between γ(β)- and α-events was used to reduce the background caused by *α*-radioactive contamination in the cadmium tungstate scintillators due to the presence of radionuclides of the ^{238}U and ^{232}Th series. The optimal filter method was used for this purpose [31]. For each pulse, its numerical characteristic, the shape indicator (*SI*), was calculated as follows [32]:

$$SI = \sum_k f\left(t_k\right) P\left(t_k\right) / \sum_k f\left(t_k\right), \qquad (4)$$

where $f(t_k)$ is the pulse amplitude value at time t_k (k is channel number); $P\left(t_k\right) = \{\overline{f_\alpha}\left(t\right) - \overline{f_\gamma}\left(t\right)\} / \left(\overline{f_\alpha}\left(t\right) + \overline{f_\gamma}\left(t\right)\right)$ is the weighting function; $\overline{f_\alpha}\left(t\right)$ and $\overline{f_\gamma}\left(t\right)$ are reference pulse shapes for α-particles and γ-quanta (β-particles). The distributions of *SI* for *γ*-quanta (β-particles) and α-particles are well described by Gaussian functions. The energy dependence of the *SI* parameter and its standard deviation were determined for α-particles from the decay of α-active nuclei in the scintillators and for γ(β)-events from calibration measurements with ^{228}Th, ^{22}Na, and ^{60}Co γ-sources.

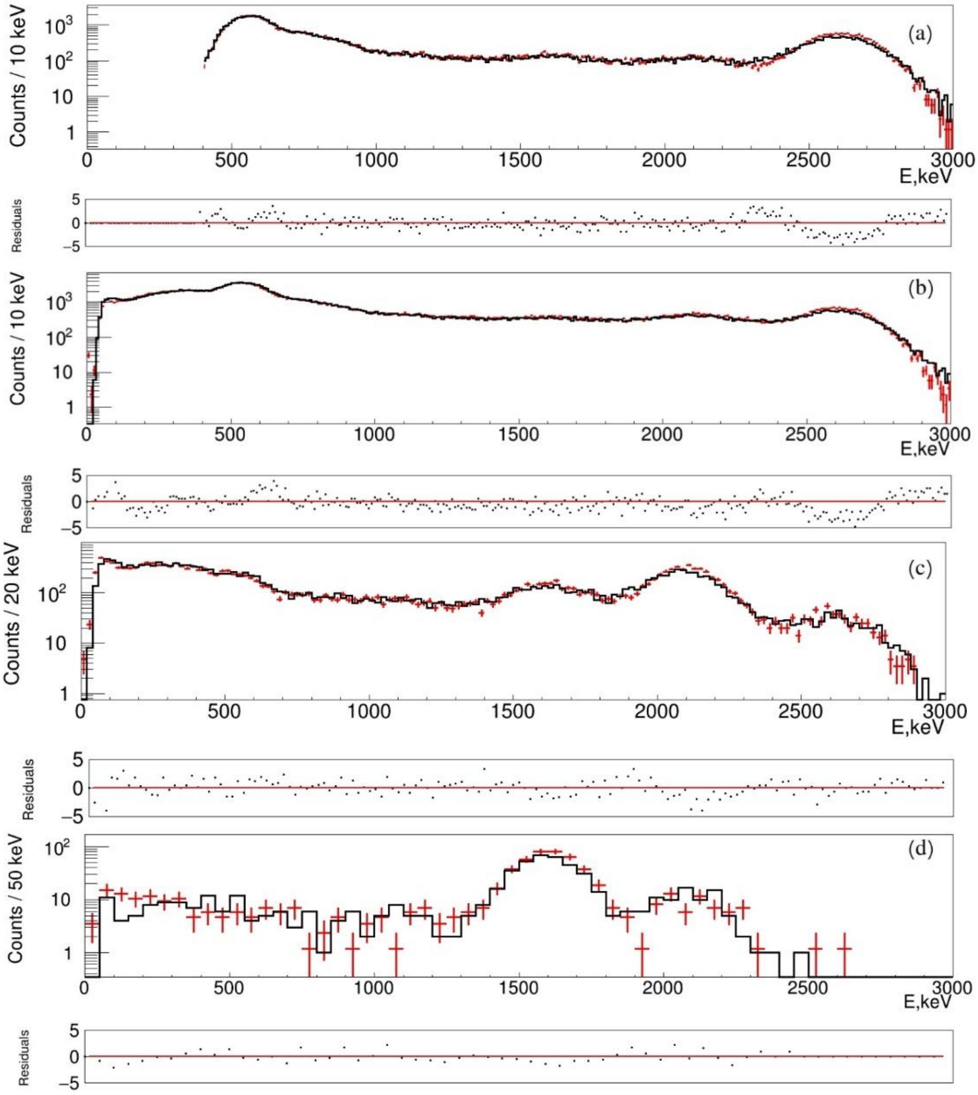

Fig. 8. Energy spectra of ^{228}Th γ-ray source measured by the $^{106}CdWO_4$ detector (black histograms) in anticoincidence mode (*a*), in coincidence with the event(s) in the $CdWO_4$ counters (*b*), in coincidence with energy 511 keV in at least one of the $CdWO_4$ counters (*c*) and in coincidence with energy 511 keV in both $CdWO_4$ detectors (*d*). The Monte Carlo models are shown by red markers. The residuals defined as (experiment – model)/uncertainties are shown below each spectrum. (See color Figure on the journal website.)

A dedicated data-taking run was carried out with the $CdWO_4$ counters for 588 h to measure the energy spectra of α-events. Fig. 9 shows the obtained dependence of *SI* on energy for one of the $CdWO_4$ detectors and the separated γ(β)- and α-event spectra after applying the pulse-shape discrimination.

The use of the optimal filter method is suitable for the statistical separation of α-particles from γ-rays (β-particles), rejection of events from the ^{212}Bi-^{212}Po decay sub-chain of ^{232}Th, PMT noises, overlapping signals, events in $^{106}CdWO_4$ plus signals in the plastic scintillator, etc. Fig. 9 shows the results of applying this method to background data collected by the $^{106}CdWO_4$ detector over 648 days. The best separation between α- and γ(β)-events is observed in the energy range of (800 - 1500) keV, where α-events from the decays of ^{232}Th and ^{238}U and their daughters are expected.

3.2. Time-amplitude analysis of ^{228}Th daughters

Time-amplitude analysis was used to determine the activity of ^{228}Th in the $CdWO_4$ and $^{106}CdWO_4$ crystals. α-events corresponding to the fast decay chain in the ^{232}Th family were selected: ^{224}Ra (Q_α = = 5.79 MeV, $T_{1/2}$ = 3.66 d) → ^{220}Rn (Q_α = 6.41 MeV, $T_{1/2}$ = 55.6 s) → ^{216}Po (Q_α = 6.91 MeV, $T_{1/2}$ = 0.145 s) → ^{212}Pb. They are in equilibrium with ^{228}Th in the scintillators. It should be noted that events were selected considering the quenching of energy of α-particles in the γ-scale of the detectors, which is described by the so-called α/γ-ratio [33]. First, we selected all event pairs within an energy interval 0.7 - 1.5 MeV in the time interval 0.026 - 1.000 s to analyze the decay chain ^{220}Rn → ^{216}Po → ^{212}Pb. The efficiency of the ^{216}Po α-decay events selection in this time interval was 87.5 %, while the pulse-shape

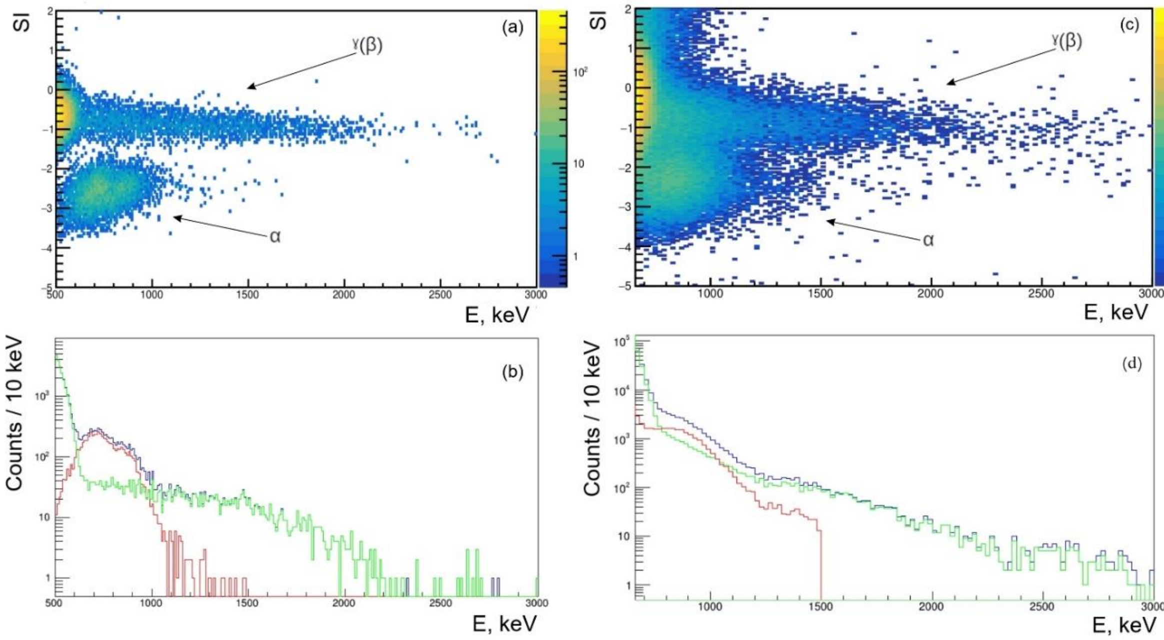

Fig. 9. The dependence of the shape indicator on energy obtained for one of the $CdWO_4$ (*a*) and for $^{106}CdWO_4$ (*c*). The figure shows the separation of signals from β(γ)- and α-particles. Spectra measured by one of the $CdWO_4$ (*b*) and $^{106}CdWO_4$ (*d*) detectors (blue), and their γ(β)-components (green) and α-components (red) selected using the optimal filter method. (See color Figure on the journal website.)

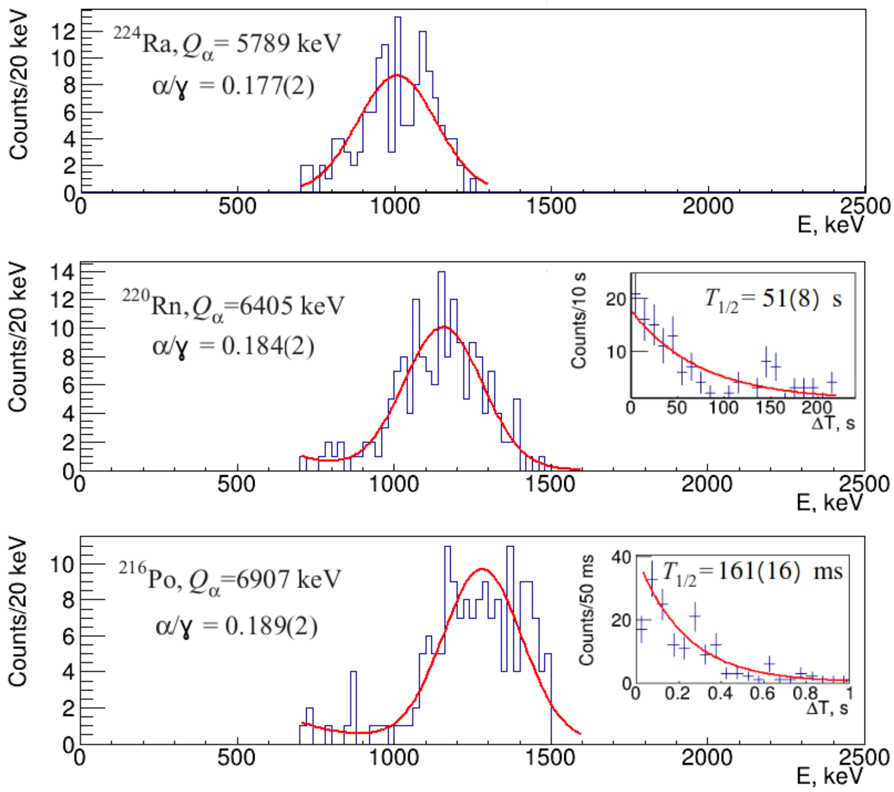

Fig. 10. Energy spectra of α events of ^{224}Ra, ^{220}Rn, and ^{216}Po selected by the time-amplitude analysis of the data accumulated over 15573 h with the $^{106}CdWO_4$ detector. The obtained half-lives (shown in the insets) of ^{216}Po (161 ± 16 ms) and ^{220}Rn (51 ± 8 s) are in agreement with the Table values $T_{1/2}$ = 0.145 s and $T_{1/2}$ = 55.6 s [34]. (See color Figure on the journal website.)

selection efficiency was 94.3 %. The activity of ^{228}Th in the $^{106}CdWO_4$ crystal was calculated to be 0.0174(14) mBq/kg. The events of the decay of the mother α active ^{224}Ra in the same energy interval were searched for in the time interval 0 - 222 s (93.7 % of ^{224}Ra→^{220}Rn chain) before the ^{220}Rn → ^{216}Po events selected in the previous step. The obtained energy spectra of α-events in the $^{106}CdWO_4$

detector from the ^{224}Ra $\rightarrow ^{220}$Rn $\rightarrow ^{216}$Po$\rightarrow ^{212}$Pb chain and the time distributions for the ^{220}Rn$\rightarrow ^{216}$Po and ^{216}Po$\rightarrow ^{212}$Pb decays are shown in Fig. 10. A similar analysis for the $CdWO_4$ counters with the shape indicator selection efficiency 99.7 % and the time interval 0.026 - 1.4 s (88.2 % of ^{216}Po decays) gives an average activity of ^{228}Th 0.012(2) mBq/kg.

The positions of the three α-peaks, selected by the time-amplitude analysis in the γ-scale of the $^{106}CdWO_4$ detector, were used to obtain the following dependence of the α/γ-ratio on the energy of α-particles (E_α) in the range 5.7 - 6.9 MeV: $\alpha/\gamma = 0.12(2) + 0.011(2)\cdot E_\alpha$ (where E_α is in MeV). The dependence agrees with the data obtained for the $^{106}CdWO_4$ scintillation detector in [17].

3.3. Analysis of α-spectra measured by $CdWO_4$ counters

To determine α-activities of ^{232}Th and ^{238}U daughters in the $CdWO_4$ crystal scintillators, the α-spectrum selected with the help of the pulse-shape discrimination was analyzed. The α/γ-ratio depends on the direction of α-particles relative to the $CdWO_4$ crystal axes, therefore the energy resolution for α-particles is worse than for γ-quanta [35]. As a result, we cannot observe individual peaks from the α-decays of U/Th daughters in the spectrum. To identify α-active nuclides, a simple model built of Gaussian functions was used to fit the spectrum in an energy interval of 450 - 1500 keV. The fit model consisted of five independent sub-chains of ^{238}U (^{238}U$\rightarrow ^{234}$Th; ^{234}U$\rightarrow ^{230}$Th; ^{230}Th$\rightarrow ^{226}$Ra; ^{226}Ra$\rightarrow ^{210}$Pb; ^{210}Pb$\rightarrow ^{206}$Pb) and two sub-chains of ^{232}Th (^{232}Th$\rightarrow ^{228}$Ra and ^{228}Th$\rightarrow ^{208}$Pb), each having its own activity. A fit result of the α spectrum measured by $CdWO_4$ is shown in Fig. 11. The activities of U/Th daughters determined from approximation are presented in the Table. The dependence of the α/γ-ratio on the energy of the α-particles (E_α) in the energy interval 470 - 1500 keV was estimated from the fit as $\alpha/\gamma = 0.08(1) + 0.015(2)\cdot E_\alpha$.

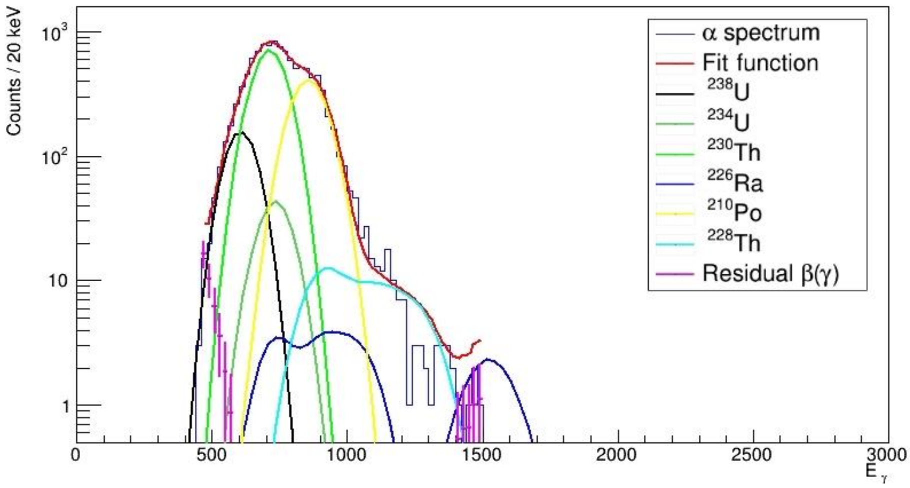

Fig. 11. Energy spectra of α-events in γ-scale selected by the pulse-shape analysis of the data accumulated with the $CdWO_4$ counters for 588 h in a dedicated run (blue histogram). Contribution of U/Th daughters sub-chains, fit function and residual β(γ)-distribution are shown by different colors (see legend). (See color Figure on the journal website.)

Radioactive contamination (mBq/kg) of the low-background setup components estimated using the approximation of the energy spectra shown in Fig. 13

Setup components	^{238}U	^{234}U	^{230}Th	^{226}Ra	^{210}Pb	^{232}Th	^{228}Ra	^{228}Th	^{40}K	^{176}Lu	^{56}Co	^{60}Co
$^{106}CdWO_4$	0.60(2)			0.015(6)	<0.3		<0.01	0.0174(14)*	<0.19	1.71(5)		
$CdWO_4$	0.29(7)†	<0.2†	1.40(7)†	<0.002†	0.89(4)†	<0.01†	<0.07	0.012(2)*	1.2(3)			
Plastic scintillator	<4.8			<3.2	<4.9		<2	<0.9	<3.9			
Optical contact	<23			<32	<14		<5	<8	<98			
Teflon tape	<2.6			<1.6	<12		<4.5	<2	<6.6			
Teflon details	<1.3			<0.9	<8.2		<3.2	<3.3	<4.3			
Quartz l. g. for $CdWO_4$	<0.6			<1.4	<1.4		<0.4	<0.3	<1.4			
Quartz l. g. for $^{106}CdWO_4$	<4.2			<7.3	<13		<7.3	<11	<16			

Continuation of the Table

Setup components	^{238}U	^{234}U	^{230}Th	^{226}Ra	^{210}Pb	^{232}Th	^{228}Ra	^{228}Th	^{40}K	^{176}Lu	^{56}Co	^{60}Co
Internal copper	<22			<0.4	<18		<1.4	<0.03	<0.9		<0.14	<0.1
External copper	<15			<0.4			<3.1	<0.05	<0.4			
PMTs for $CdWO_4$	<900			<900			<300	<110	<1200			
PMT for $^{106}CdWO_4$	<44			<9.7			<23	<27	<41			

N o t e. Upper limits are given at 90 % confidence level, values are given with 68 % statistical uncertainty. Only statistical uncertainties are shown. Activities labeled by (*) were determined by using the time-amplitude analysis, the values marked by (†) were determined by the α-spectrum analysis.

3.4. Background model

To reduce the background further, a selection of coincidence and anticoincidence events in the $^{106}CdWO_4$ and $CdWO_4$ detectors was applied. The background was reduced for energies greater than ~ 0.8 MeV by using an anti-coincidence condition with the $CdWO_4$ counters. Further background reduction was achieved by selecting events in the $^{106}CdWO_4$ detector in coincidence with at least one of the $CdWO_4$ counters with energy deposition in the range 511 ± 2σ keV, where σ is the energy resolution of the $CdWO_4$ counters for 511 keV γ-quanta. Selecting events in the $^{106}CdWO_4$ detector in coincidence with events in the energy range 511 ± 2σ keV in both $CdWO_4$ counters gives only three events, indicating a low level of background and high sensitivity of the experiment. Fig. 12 shows the background spectra under the different selection conditions.

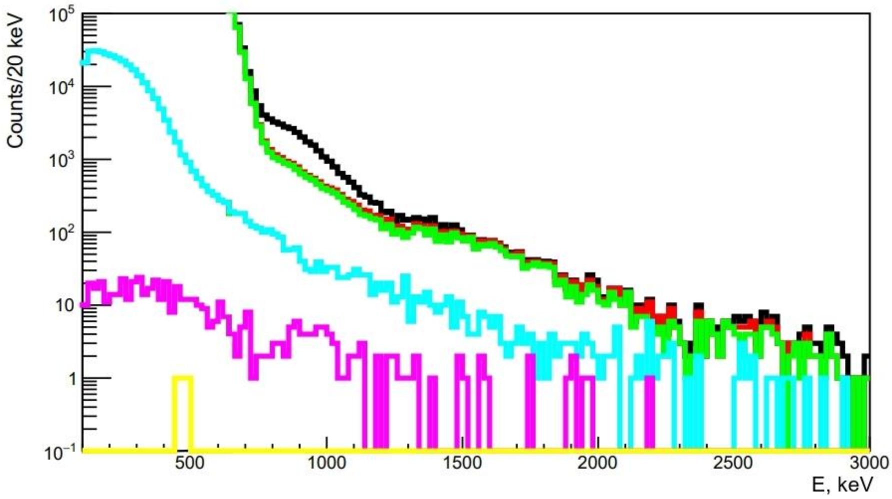

Fig. 12. Energy spectra measured by the $^{106}CdWO_4$ detector for 15573 h. In particular, the following spectra are shown: energy spectrum without cuts (black), spectrum of γ(β)-events selected by the pulse-shape discrimination (see Section 3.1., red), γ(β)-events in anticoincidence with the $CdWO_4$ detectors (green), γ(β)-events in coincidence with $CdWO_4$ detectors (cyan), γ(β)-events in coincidence with an event in at least one of the $CdWO_4$ detectors in the energy range 511 ± 2σ keV (violet), γ(β)-events in coincidence with events in both $CdWO_4$ detectors in the energy range 511 ± 2σ keV (yellow). (See color Figure on the journal website.)

The energy spectrum for energies below ~ 0.8 MeV is mainly due to β-decays of ^{113m}Cd and ^{113}Cd. To describe the experimental data above 0.8 MeV, a background model was constructed, which includes radioactive contaminations in the $^{106}CdWO_4$ and $CdWO_4$ crystals, and in the components of the setup. The internal contaminations of the $^{106}CdWO_4$ crystal above 0.8 MeV consist of the following components:

– ^{40}K, ^{228}Ra→^{228}Th, ^{228}Th→^{208}Pb, ^{238}U→^{234}U, ^{226}Ra→^{210}Pb and ^{210}Pb→^{206}Pb, with activities estimated in the previous stages of the experiment [17]. In addition, peaks with energies of 202 keV and 307 keV were observed in the data collected with the $^{106}CdWO_4$ detector, which can be explained by the presence of ^{176}Lu in the crystal. Therefore, a distribution for this radionuclide was added to the background model;

– the residual distribution of α-particles from decays of ^{232}Th, ^{238}U, and their daughters;

– the spectrum of the two-neutrino 2β-decay of ^{116}Cd with a half-life of $T_{1/2} = 2.63 \cdot 10^{19}$ years [36].

To model the background from the setup details, distributions were simulated for the following sources:

– ^{40}K, ^{228}Ra→^{228}Th, ^{228}Th→^{208}Pb, ^{238}U→^{234}U, ^{226}Ra→^{210}Pb, and ^{210}Pb→^{206}Pb in the $CdWO_4$ crystals, plastic scintillator, optical contact material, Teflon details and quartz light guides;

– ^{40}K, ^{228}Ra→^{228}Th, ^{228}Th→^{208}Pb, ^{238}U→^{234}U, and ^{226}Ra→^{210}Pb in the external copper and PMTs;

– ^{40}K, ^{228}Ra→^{228}Th, ^{228}Th→^{208}Pb, ^{238}U→^{234}U, ^{226}Ra→^{210}Pb, ^{210}Pb→^{206}Pb, ^{56}Co, and ^{60}Co in the internal copper.

All the mentioned radionuclides were simulated using the Monte Carlo package EGSnrc [30] with the initial kinematics provided by the event generator DECAY0 [37]. The residual distribution of events from the α decays of ^{232}Th and ^{238}U and their daughters in the $^{106}CdWO_4$ crystal was constructed from the experimental data using the pulse-shape discrimination technique described in Section 3.1.

The obtained models were used for the description of the following five experimental spectra:

1. γ(β)-spectrum measured by the $^{106}CdWO_4$ detector in the energy interval of 850 - 3000 keV in anticoincidence with the $CdWO_4$ counters;

2. γ(β)-spectrum measured by the $^{106}CdWO_4$ detector in the energy interval of 600 - 3000 keV in coincidence with events in the $CdWO_4$ counters with energy above 80 keV;

3. γ(β)-spectrum measured by the $^{106}CdWO_4$ detector in the energy interval of 600-3000 keV in coincidence with events in at least one of the $CdWO_4$ counters in the energy interval 511 ± 2σ keV;

4. γ(β)-spectrum measured by the $CdWO_4$ detectors in the energy interval of 600 - 3000 keV in coincidence with events in $^{106}CdWO_4$ with energy deposition above the threshold;

5. γ(β)-spectrum measured by the $CdWO_4$ detectors in the energy interval of 150 - 3000 keV in coincidence with events in $^{106}CdWO_4$ with energy deposition above 500 keV (to identify ^{176}Lu peaks).

For each selection condition, its selection efficiency related to the pulse-shape analysis and the time resolution of the $^{106}CdWO_4$ and $CdWO_4$ detectors were determined. The obtained efficiency was used to modify the Monte Carlo models in order to align them with the collected data. The corresponding models were fitted to the five spectra. The quality of the approximation is rather high (χ^2 = 647 for 391 degrees of freedom). The fit results are shown in Fig. 13.

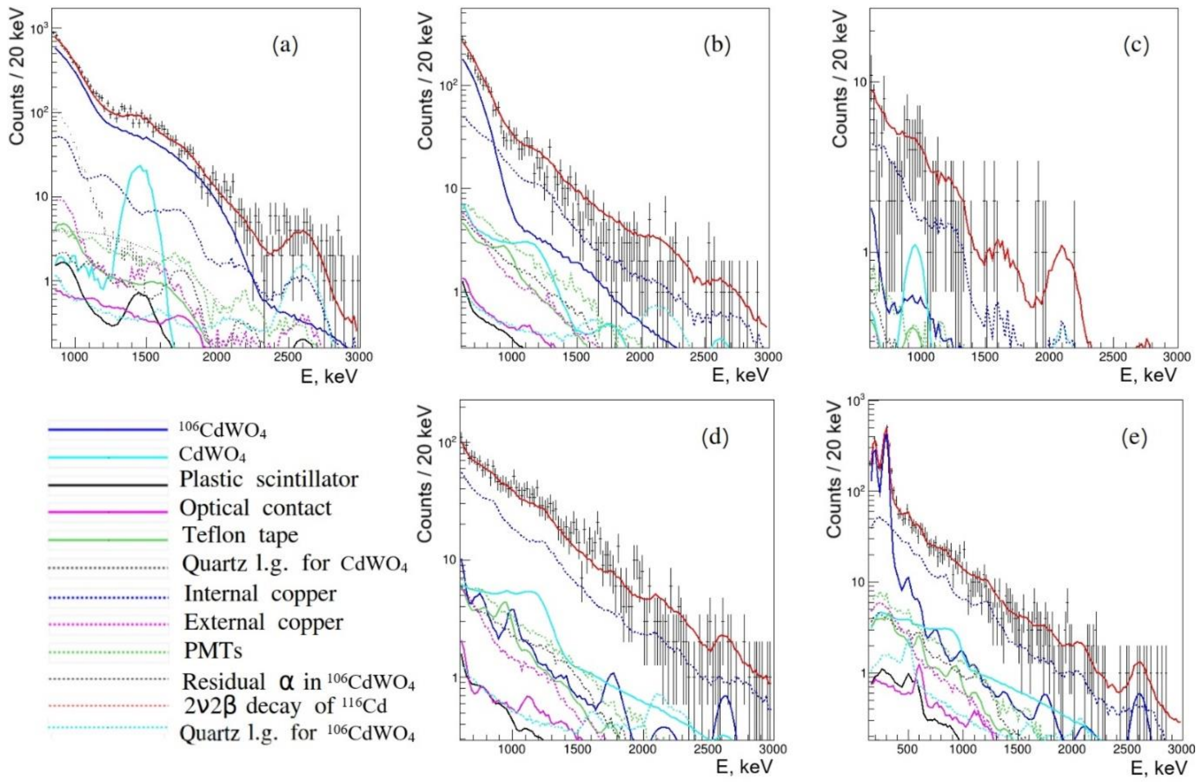

Fig. 13. Results of the combined approximation of γ(β)-spectra measured by detectors: *a* - $^{106}CdWO_4$ in anticoincidence with the $CdWO_4$ detectors; *b* - $^{106}CdWO_4$ in coincidence with event(s) in the $CdWO_4$ counters with energy greater than 80 keV; *c* - $^{106}CdWO_4$ in coincidence with event(s) in at least one of the $CdWO_4$ detectors with energy in the interval 511 ± 2σ keV; *d* - $CdWO_4$ in coincidence with events in $^{106}CdWO_4$ above the threshold 80 keV; *e* - $CdWO_4$ in coincidence with events in $^{106}CdWO_4$ with energy deposition greater than 500 keV for the purpose of ^{176}Lu peaks identification. The red line represents the background model. The contributions from the contamination of different components of the setup are shown separately (see legend). (See color Figure on the journal website.)

In Fig. 13, *e*, two peaks with energies of 202 and 307 keV are clearly visible. The peaks can be explained by contamination of the $^{106}CdWO_4$ crystal scintillator by ^{176}Lu that β-decay to the 597-keV 6^+ level of ^{176}Hf. The contaminations of the $CdWO_4$ crystals by radionuclides ^{238}U, ^{210}Pb, and ^{228}Th were determined by the analysis of the α-distribution, which is well separated from the γ(β)-events by the optimal filter method (see Section 3.1). The fit of the γ(β)-spectra makes it possible to estimate the radioactive contamination of the low-background setup materials. The obtained results are presented in the Table.

3.5. Sensitivity of the experiment to 2ε-, εβ⁺-, and 2β⁺-processes in ¹⁰⁶Cd

There are no peculiarities in the experimental data that could be attributed to 2β-processes in ^{106}Cd. Lower limits on the half-life of ^{106}Cd relative to different channels and modes of 2β-decay can be estimated using the formula:

$$\lim T_{1/2} = N \cdot \ln 2 \cdot \eta_{sel} \cdot \eta_{det} \cdot t / \lim S, \qquad (5)$$

where N is the number of ^{106}Cd nuclei in the $^{106}CdWO_4$ crystal ($2.42 \cdot 10^{23}$), η_{det} is the detection efficiency of the decay process (calculated as a ratio of the number of events in the simulated distribution to the number of generated events), η_{sel} is the selection efficiency (by using the optimal filter method, time coincidence, and energy window), t is the measurement time, and lim S is a maximal number of events of the sought-for effect that can be excluded with a given confidence level. The detector responses to different modes and channels of the 2β-decay of ^{106}Cd were simulated using the Monte Carlo package EGSnrc with the initial kinematics provided by the event generator DECAY0. Approximately $5 \cdot 10^6$ events were generated for each decay mode.

To estimate the sensitivity of the experiment to some 2β-processes in ^{106}Cd, the data were analyzed under various selection conditions. An example of such analysis for the $0\nu\varepsilon\beta^+$ and $0\nu2\beta^+$ decays of ^{106}Cd to the ground state of ^{106}Pd, using the energy spectrum of the $^{106}CdWO_4$ detector in coincidence with an energy release 511 ± 2σ keV in at least one of the $CdWO_4$ counters, is shown in Fig. 14. To derive a limit on the effect searched for, the number of measured events was compared to the expected background. The expected background was estimated from the fit shown in Fig. 13. In the energy interval of 1300 - 2400 keV, the expected background is 45 counts, while there are 18 events in the measured spectrum, which leads to lim $S = 1.5$ with a 90 % confidence level according to Feldman and Cousins' recommendations [38]. Using a more conservative approach that considers only the number of observed events (experimental sensitivity [38]), we obtain a value of lim S = 8.7 counts at 90 % confidence level.

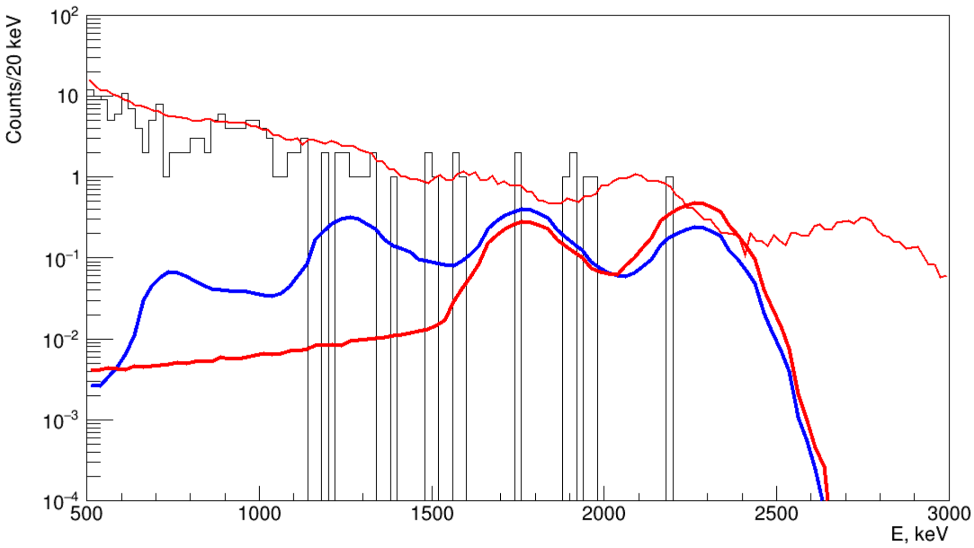

Fig. 14. The energy spectrum measured by the $^{106}CdWO_4$ detector in coincidence with events with energy 511 ± 2σ keV in at least one of the $CdWO_4$ counters. The red thin line represents the background model. The blue bold line corresponds to the $0\nu2\beta^+$-decay of ^{106}Cd to the ground state of ^{106}Pd with $T_{1/2}^{0\nu2\beta} = 8.4 \cdot 10^{21}$ years. The red bold line corresponds to the $0\nu\varepsilon\beta^+$-decay of ^{106}Cd to the ground state of ^{106}Pd with $T_{1/2}^{0\nu\varepsilon\beta} = 1.1 \cdot 10^{22}$ years. (See color Figure on the journal website.)

For $0\nu\varepsilon\beta^+$ decay of ^{106}Cd to the ground state of ^{106}Pd, $\eta_{det} = 0.37802$, $\eta_{sel} = 0.8116$ is calculated as a product of the selection efficiencies of the optimal filter method for $^{106}CdWO_4$ (0.9493) and for $CdWO_4$ (0.9973), selection based on the time resolution in the time interval of –20...+40 ns (0.9580), selection of events in $CdWO_4$ with energy of 511 ± 2σ keV (0.9545), and selection of events in the energy interval of 1300 - 2400 keV (0.9375). Using the formula (5) and the "experimental sensitivity" approach we calculate a half-life limit as $\lim T_{1/2}^{0\nu\varepsilon\beta} = 1.1 \cdot 10^{22}$ years.

For $0\nu 2\beta^+$-decay of ^{106}Cd to the ground state of ^{106}Pd, η_{det} = 0.39386, η_{sel} = 0.6191. By using the "experimental sensitivity" approach a similar analysis gives $\lim T_{1/2}^{0\nu 2\beta} = 8.4 \cdot 10^{21}$ years.

The highest experimental sensitivity to the $2\nu\varepsilon\beta^+$-decay channel can be achieved using the data of the $^{106}CdWO_4$ detector in coincidence with annihilation γ-ray quanta in both the $CdWO_4$ counters. Thanks to a very low background level, only three events were detected in this regime (Fig. 15). Similarly, to the analysis of the spectrum in coincidences with at least one 511 keV γ-ray, a comparison of the number of measured events with the expected background was applied. The background was obtained from the results of the combined approximation. In the energy interval 100 - 1400 keV, the background model gives 6.2 counts confirming a reasonably correct background modelling. According to the recommendations [38], lim S = 5.6 counts with a 90 % confidence level. Considering the detection (0.0405) and selection (0.6991) efficiencies for the $2\nu\varepsilon\beta^+$-decay of ^{106}Cd to the ground state of ^{106}Pd, we obtain lim $T_{1/2}$ = $1.5 \cdot 10^{21}$ years.

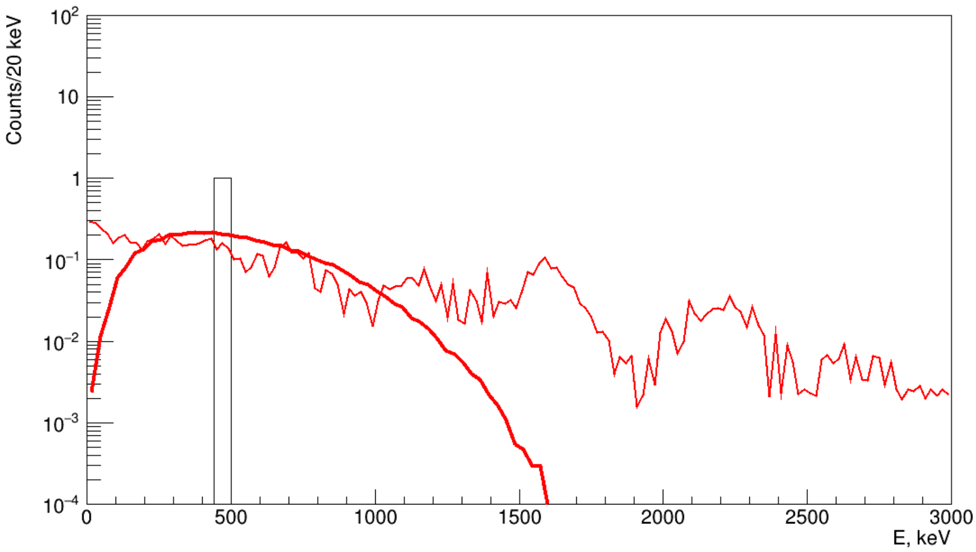

Fig. 15. Energy spectrum measured by the $^{106}CdWO_4$ detector in coincidence with annihilation γ-ray quanta in both $CdWO_4$ counters. The red thin line represents the background model. The model of the $2\nu\varepsilon\beta^+$-decay of ^{106}Cd to the ground state of ^{106}Pd with $T_{1/2} = 1.5 \cdot 10^{21}$ years is shown by solid red line. (See color Figure on the journal website.)

Another way to estimate the half-life limit on the decays is to approximate the energy spectra with a background model plus the effect searched for. For each selection condition, Monte Carlo models were constructed taking into account the detection and selection efficiencies, multiplied by a parameter obtained from the combined fit result. Accordingly, formula (5) can be modified as follows:

$$\lim T_{1/2} = N \cdot ln2 \cdot t / \lim A, \qquad (6)$$

where A is the number of decays of the 2β-process searched for which can be excluded by the fit procedure at 90 % C.L. For the $0\nu 2\varepsilon$-decay of ^{106}Cd to the ground state of ^{106}Pd the result of the approximation is shown in Fig. 16. The approach gives a value of the parameter A = 186 ± 92, which is no evidence of the effect. According to the recommendations [38], we adopt lim A = 337 events at 90 % confidence level. Using the formula (6), we obtain a lower half-life limit on the $0\nu 2\varepsilon$ decay of ^{106}Cd to the ground state of ^{106}Pd, $T_{1/2} \geq 8.9 \cdot 10^{20}$ years, which is almost 1.5 times higher than the previous result [22].

4. Conclusions

An experiment to search for 2β-decay of ^{106}Cd with the help of enriched $^{106}CdWO_4$ crystal scintillator in (anti)coincidences with two large volume $CdWO_4$ scintillators in close geometry is running at the Gran Sasso underground laboratory of the National Institute for Nuclear Physics (Italy). To take into account the energy scale shift of the $^{106}CdWO_4$ detector due to the PMT instability, correction methods using the edge of the β-spectrum of ^{113m}Cd and the results of calibration measurements were developed. The main time and spectroscopic characteristics of the detector system were determined. Comparison of the experimental data obtained in the calibration measurements with γ-ray sources with the Monte Carlo simulations demonstrated a good

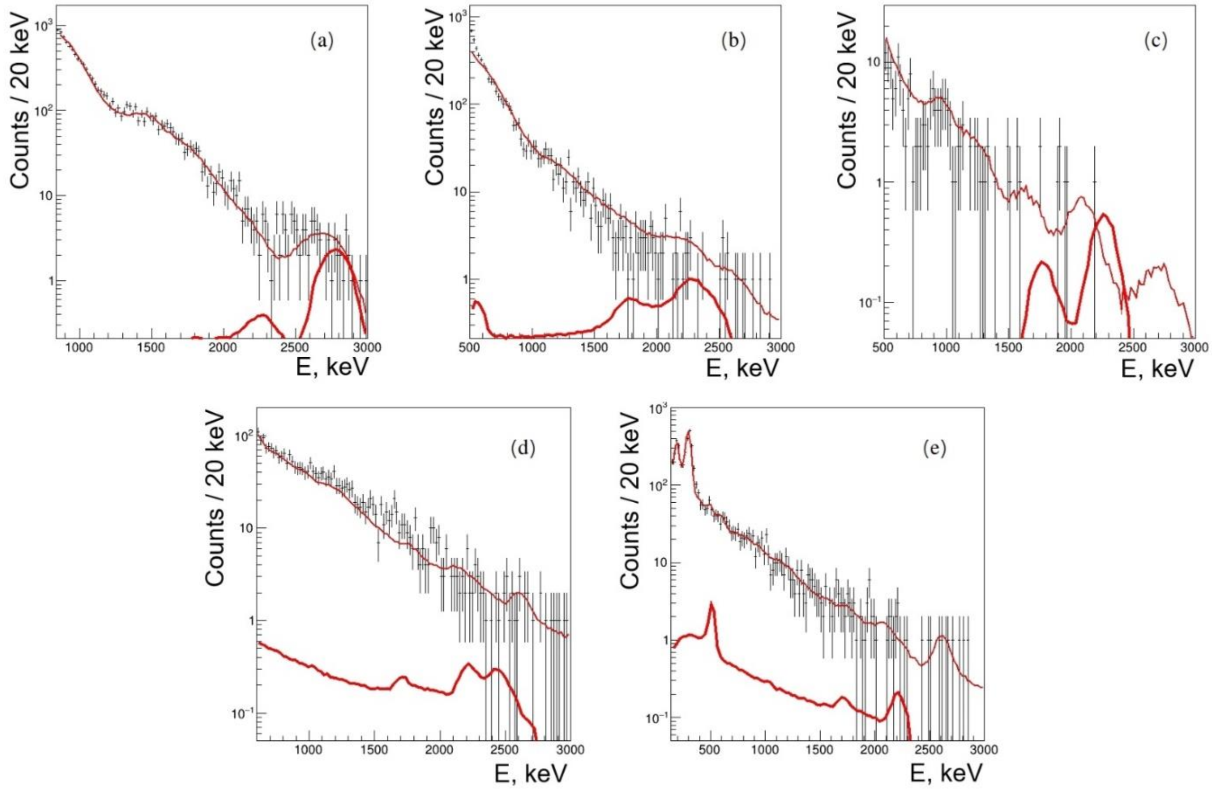

Fig. 16. The result of the combined approximation of the γ(β)-spectra by the background model (red line) plus the effect of the 0ν2ε-decay of ^{106}Cd to the ground state of ^{106}Pd with $T_{1/2}$ = 8.9·10^{20} years (red bold line). *a* - ^{106}CdWO$_4$ in anticoincidence with the CdWO$_4$ detectors; *b* - ^{106}CdWO$_4$ in coincidence with events in the CdWO$_4$ detectors with energy above 80 keV; *c* - ^{106}CdWO$_4$ in coincidence with events in at least one of the CdWO$_4$ detectors with energy 511 ± 2σ keV; *d* - CdWO$_4$ in coincidence with events in ^{106}CdWO$_4$; *e* - CdWO$_4$ in coincidence with events in ^{106}CdWO$_4$ with an energy deposition above 500 keV. (See color Figure on the journal website.)

agreement and allowed us to determine the energy thresholds of the detector system accurately. The background model was constructed taking into account almost all components of the detector system. The data taken over 1.777 years were fitted in different coincidence (anticoincidence) conditions; the radioactive contamination of the setup materials was estimated. The radioactive contaminations of the ^{106}CdWO$_4$ and CdWO$_4$ scintillation crystals were determined using time-amplitude and pulse-shape analyses and fit of the energy spectra in different (anti)coincidences modes. The experimental sensitivity to several 2β-decay processes in ^{106}Cd to the ground state of ^{106}Pd was estimated in different conditions of (anti)coincidences as: $T_{1/2}^{0\nu2\varepsilon} > 8.9\times$ $\times10^{20}$ years, $T_{1/2}^{0\nu2\beta} > 8.4\cdot10^{21}$ years, $T_{1/2}^{2\nu\varepsilon\beta} > 1.5\times$ $\times10^{21}$ years and $T_{1/2}^{0\nu\varepsilon\beta} > 1.1\cdot10^{22}$ years. In the beginning of 2022, the experimental set-up was upgraded by changing the ^{106}CdWO$_4$ and CdWO$_4$ counters PMTs and installation of a channel for periodical calibration with γ-ray sources without opening the set-up shielding and switching off the high voltage on the PMTs. The measurements and data analysis are in progress to improve the experimental sensitivity by using the entire data accumulated from the beginning of the experiment in November 2019.

We express our gratitude to the Armed Forces of Ukraine which gave us the opportunity to perform this study during the military aggression of the Russian Federation against Ukraine. This work was supported in part by the National Research Foundation of Ukraine (Grant No. 2020.02/0011), and by the National Academy of Sciences of Ukraine (Reg. No. 0123U103151). V. V. Kobychev is grateful to the Georgia Institute of Technology for kind support within the Universities for Ukraine (U4U) Non-Residential Fellowship Program. F. A. Danevich, O. G. Polischuk, and V. I. Tretyak thank the INFN, sezione di Roma “Tor Vergata”, sezione di Roma “La Sapienza”, Laboratori Nazionali del Gran Sasso and the people of the DAMA group for the great support and hospitality in the difficult times during the Russian invasion of Ukraine.

REFERENCES

1. A. Giuliani, A. Poves. Neutrinoless Double-Beta Decay. AHEP 2012 (2012) 857016.
2. M. Agostini et al. Toward the discovery of matter creation with neutrinoless double-beta decay. Rev. Mod. Phys. 95 (2023) 025002.
3. O. Cremonesi, M. Pavan. Challenges in Double Beta Decay. AHEP 2014 (2014) 951432.
4. E. Bossio, M. Agostini. Probing Beyond the Standard Model Physics with Double-beta Decays. arXiv:2304.07198v1 [hep-ex] (2023).
5. S.M. Bilenky, C. Giunti. Neutrinoless double-beta decay: A probe of physics beyond the Standard Model. Int. J. Mod. Phys. A 30 (2015) 1530001.
6. S. Dell'Oro et al. Neutrinoless Double Beta Decay: 2015 Review. AHEP 2016 (2016) 2162659.
7. M.J. Dolinski, A.W.P. Poon, W. Rodejohann. Neutrinoless double beta decay: Status and prospects. Annu. Rev. Nucl. Part. Sci. 69 (2019) 219.
8. T. Asaka, M. Shaposhnikov. The νMSM, dark matter and baryon asymmetry of the universe. Phys. Lett. B 620 (2005) 17.
9. F.F. Deppisch et al. Neutrinoless double beta decay and the baryon asymmetry of the Universe. Phys. Rev. D 98 (2018) 055029.
10. A.S. Barabash. Precise Half-Life Values for Two-Neutrino Double-β Decay: 2020 Review. Universe 6 (2020) 159.
11. R. Saakyan. Two-Neutrino Double-Beta Decay. Annu. Rev. Nucl. Part. Sci. 63 (2013) 503.
12. A.P. Meshik et al. Weak decay of ^{130}Ba and ^{132}Ba: Geochemical measurements. Phys. Rev. C 64 (2001) 035205.
13. M. Pujol et al. Xenon in Archean barite: Weak decay of ^{130}Ba, mass-dependent isotopic fractionation and implication for barite formation. Geochim. Cosmochim. Acta 73 (2009) 6834.
14. Yu.M. Gavrilyuk et al. Indications of 2ν2K capture in ^{78}Kr. Phys. Rev. C 87 (2013) 035501.
15. S.S. Ratkevich et al. Comparative study of the double-K-shell-vacancy production in single- and double-electron-capture decay. Phys. Rev. C 96 (2017) 065502.
16. E. Aprile et al. (XENON Collaboration). Search for new physics in electronic recoil data from XENONnT. Phys. Rev. Lett. 129 (2022) 161805.
17. P. Belli et al. Search for double-β decay processes in ^{106}Cd with the help of a $^{106}CdWO_4$ crystal scintillator. Phys. Rev. C 85 (2012) 044610.
18. M. Wang et al. The AME2020 atomic mass evaluation (II). Tables, graphs and references. Chin. Phys. C 45 (2021) 030003.
19. J. Meija et al. Isotopic composition of the elements 2013. (IUPAC Technical Report). Pure Appl. Chem. 88 (2016) 293.
20. P. Belli et al. Development of enriched $^{106}CdWO_4$ crystal scintillators to search for double β decay processes in ^{106}Cd. Nucl. Instrum. Meth. A 615 (2010) 301.
21. P. Belli et al. Search for 2β decay in ^{106}Cd with an enriched $^{106}CdWO_4$ crystal scintillator in coincidence with four HPGe detectors. Phys. Rev. C 93 (2016) 045502.
22. P. Belli et al. Search for Double Beta Decay of ^{106}Cd with an Enriched $^{106}CdWO_4$ Crystal Scintillator in Coincidence with $CdWO_4$ Scintillation Counters. Universe 6 (2020) 182.
23. D. De Frenne, A. Negret. Nuclear data sheets for A = 106. Nucl. Data Sheets 109 (2008) 943.
24. R. Bernabei et al. First results from DAMA/LIBRA and the combined results with DAMA/NaI. Eur. Phys. J. C 56 (2008) 333.
25. X. Mougeot. Reliability of usual assumptions in the calculation of β and ν spectra. Phys. Rev. C 91 (2015) 055504.
26. H. Primakoff, S.P. Rosen. Double beta decay. Rep. Prog. Phys. 22 (1959) 121.
27. L. Cadamuro et al. Characterization of the Hamamatsu R11265-103-M64 multi-anode photomultiplier tube. Journal of Instrumentation 9 (2014) 06021.
28. M. Calvi et al. Characterization of the Hamamatsu H12700A-03 and R12699-03 multi-anode photomultiplier tubes. Journal of Instrumentation 10 (2015) 09021.
29. L.T. Tsankov, M.G. Mitev. Response of a NaI(Tl) scintillation detector in a wide temperature interval. Proceedings of the Technical University - Sofia 56(1) (2006) 160.
30. I. Kawrakow et al. The EGSnrc Code System: Monte Carlo Simulation of Electron and Photon Transport. NRCC Report PIRS-701 (Ottawa, Canada, National Research Council of Canada, 2003) 323 p.
31. E. Gatti, F. De Martini. A new linear method of discrimination between elementary particles in scintillation counters. In: Nuclear Electronics. Vol. II. Proc. of the Conf. on Nuclear Electronics, Belgrade, 15 - 20 May 1961 (Vienna, IAEA, 1962) p. 265.
32. F.A. Danevich et al. Search for 2β decay of cadmium and tungsten isotopes: Final results of the Solotvina experiment. Phys. Rev. C 68 (2003) 035501.
33. V.I. Tretyak. Semi-empirical calculation of quenching factors for ions in scintillators. Astropart. Phys. 33 (2010) 40.
34. R.B. Firestone, C.M. Baglin, S.Y. Frank Chu. *Table of Isotopes*. 8th ed. (New York, John Wiley, 1996) and CD update (1998).
35. F.A. Danevich et al. α activity of natural tungsten isotopes. Phys. Rev. C 67 (2003) 014310.
36. A.S. Barabash et al. Final results of the Aurora experiment to study 2β decay of ^{116}Cd with enriched $^{116}CdWO_4$ crystal scintillators. Phys. Rev. D 98 (2018) 092007.
37. O.A. Ponkratenko, V.I. Tretyak, Y.G. Zdesenko. Event generator DECAY4 for simulating double-beta processes and decays of radioactive nuclei. Phys. Atom. Nucl. 63 (2000) 1282.
38. G.J. Feldman, R.D. Cousins. Unified approach to the classical statistical analysis of small signals. Phys. Rev. D 57 (1998) 3873.

**П. Беллі[1,2], Р. Бернабей[1,2,*], Ф. Каппелла[3,4], В. Караччіоло[1,2], Р. Черуллі[1,2],
Ф. А. Даневич[2,5], А. Інчікчітті[3,4], Д. В. Касперович[5], В. Р. Клавдієнко[5], В. В. Кобичев[5],
А. Леончіні[1,2], В. Мерло[1,2], О. Г. Поліщук[3,5], В. І. Третяк[5,6]**

[1] *Факультет фізики Римського університету «Tor Vergata», Рим, Італія*
[2] *Національний інститут ядерної фізики, Римське відділення "Tor Vergata", Рим, Італія*
[3] *Національний інститут ядерної фізики, Римське відділення, Рим, Італія*
[4] *Факультет фізики Римського університету «La Sapienza», Рим, Італія*
[5] *Інститут ядерних досліджень НАН України, Київ, Україна*
[6] *Національний інститут ядерної фізики, Національна лабораторія Гран-Сассо, Ассерджі, Італія*

*Відповідальний автор: rita.bernabei@roma2.infn.it

НИЗЬКОФОНОВИЙ ЕКСПЕРИМЕНТ ПО ПОШУКУ ПОДВІЙНОГО БЕТА-РОЗПАДУ ^{106}Cd ІЗ СЦИНТИЛЯТОРОМ $^{106}CdWO_4$

Експеримент з пошуку 2ε-, $\varepsilon\beta^+$- і $2\beta^+$-розпадів ^{106}Cd з використанням сцинтиляційного кристала вольфрамату кадмію вагою 215 г, збагаченого до 66 % ^{106}Cd ($^{106}CdWO_4$), проводиться в підземній лабораторії Гран-Сассо (Італія). Події в детекторі $^{106}CdWO_4$ реєструються в (анти)збігах з двома сцинтиляційними лічильниками $CdWO_4$ великого об'єму. Описано конструкцію детекторної системи, калібрування та фонові вимірювання, методи та результати аналізу даних для визначення основних характеристик детектора. Експериментальні дані порівнюються з результатами моделювання методом Монте-Карло для побудови моделі фону. Досліджено радіоактивне забруднення елементів установки. Чутливість експерименту наближається до рівня теоретичних передбачень для каналу $2\nu\varepsilon\beta^+$-розпаду, тоді як для інших можливих каналів 2β-розпаду вона знаходиться на рівні lim $T_{1/2} \sim 10^{21}$ - 10^{22} років.

Ключові слова: ^{106}Cd, подвійний бета-розпад, 2ε, $\varepsilon\beta^+$ і $2\beta^+$, низький фон, сцинтиляційний детектор.

Надійшла/Received 30.06.2023